

Phase diagram, ferromagnetic martensitic transformation and magnetoresponse properties of Fe-doped MnCoGe alloys

G. J. Li^a, E. K. Liu^a, H.G. Zhang^a, Y. J. Zhang^a, J. L. Chen^a, W. H. Wang^a, H. W. Zhang^a, G. H. Wu^{a,*}, S. Y. Yu^b

^a Beijing National Laboratory for Condensed Matter Physics, Institute of Physics, Chinese Academy of Science, Beijing 100190, People's Republic of China

^b School of Physics, Shandong University, Jinan 250100, People's Republic of China

Abstract

The crystal structure and magnetoresponse properties of Fe-doped MnCoGe alloys have been investigated using x-ray diffraction (XRD) and magnetic measurements. By alloying the Fe-containing isostructure compounds into MnCoGe, a magnetostructural transition from paramagnetic austenite to ferromagnetic martensite with large magnetization difference can be realized in a temperature window between the Curie temperatures of the austenite and martensite, resulting in magnetic-field-induced martensitic transformations and large magnetic-entropy changes. A structural and magnetic phase diagram of Fe-doped MnCoGe alloys has been proposed.

Keywords: Isostructural alloying, Ferromagnetic martensitic transformation, Magnetoresponse properties, Fe-doped MnCoGe alloys

1. Introduction

Ferromagnetic (FM) martensitic-transition materials have attracted increasing attention due to their magneto-responsive effects, including magnetic-field-induced martensitic transformation/strain effect^[1-3], magnetoresistance^[4, 5] and magnetocaloric effect^[6, 7], et al. For these properties, the magnetostructural coupling between structural and magnetic transition plays a crucial role. Thus, exploring materials with magnetostructural transition is of importance for fundamental science and technologic application.

The magnetic equiatomic MM'X (M, M'=transition metals, X=Si, Ge, Sn) compounds^[8-11] have become interesting research objects due to their remarkable magneto-responsive properties^[12-25]. As one of the important MM'X compounds, the stoichiometric MnCoGe alloy transforms from the Ni₂In-type hexagonal structure (space group $p6_3/mmc$, 194) to the TiNiSi-type orthorhombic structure (space group $pnma$, 62) via the martensitic transformation at about 420 K, i.e. martensitic transformation temperature (T_m). The Curie temperatures of hexagonal austenite and orthorhombic martensite are 276 K (T_C^A) and 355 K (T_C^M), respectively^[9-11]. It can be seen that T_C^M is about 80 K higher than T_C^A . Because T_m is higher than T_C^M , the martensitic transformation occurs in the paramagnetic (PM) state without a magnetostructural coupling. If lowering the T_m below T_C^M , a magnetostructural transition can occur in the magnetic region. In previous studies, a martensitic transformation between PM Ni₂In-type structure and FM TiNiSi-type structure can be obtained in a temperature window between T_C^A and T_C^M by introducing the vacancy^[17], the fourth elements^[18, 19, 21, 22, 24, 25] or pressure^[26-28] in MnCo(Ni)Ge alloys. Thus, a strong magnetostructural coupling with large magnetization difference can be realized. The previous reports indicate that the doping of Fe in Heusler alloys^[29-31], Ru-based^[32] alloys or Gd₅Ge₂Si₂^[33] can suppress the martensitic transition and stabilize the parent phases. Recently, chemically alloying the Fe-containing isostructure MnFeGe or FeNiGe alloy to Ni₂In-type MnNiGe is proved to be an effective method to manipulate the first-order martensitic transformation in a temperature window^[18]. Another study has reported the magnetocaloric effect based on a second-order magnetic transition at T_C in MnCo_{1-x}Fe_xGe alloys ($x=0-1.00$)^[34]. However, the study on the first-order martensitic transformation based on the coupling of magnetic and

structural transitions, and their magneto-responsive properties of $\text{MnCo}_{1-x}\text{Fe}_x\text{Ge}$ ($x < 0.10$) is still absent up to now.

In this work, based on the isostructural alloying method, the $\text{MnCo}_{1-x}\text{Fe}_x\text{Ge}$ and $\text{Mn}_{1-x}\text{Fe}_x\text{CoGe}$ alloys were prepared. The study on the first-order FM martensitic transformation in Fe-doped MnCoGe alloys was carried out. By Fe substitution, a temperature window between T_C^A and T_C^M and therein a martensitic transformation from PM austenite to FM martensite with large magnetization difference were realized. The magnetic-field-induced martensitic transformations and magnetocaloric effects were also investigated.

2. Experimental method

Polycrystalline ingots of $\text{MnCo}_{1-x}\text{Fe}_x\text{Ge}$ ($x = 0-0.15$) and $\text{Mn}_{1-x}\text{Fe}_x\text{CoGe}$ ($x = 0-0.10$) alloys were prepared by arc-melting high-purity metal Mn, Co, Ge and Fe with purity of 99.99% and higher under argon atmosphere. The ingots were homogenized subsequently in evacuated quartz tubes with argon at 1123 K for five days and then quenched into ice water. The X-ray diffraction (XRD) with Cu-K α was employed to characterize the crystal structures. The magnetic measurements of the samples were carried out by a superconducting quantum interference device (SQUID).

3. Results and discussion

Figure 1 (a) and (b) show the powder XRD patterns of $\text{MnCo}_{1-x}\text{Fe}_x\text{Ge}$ and $\text{Mn}_{1-x}\text{Fe}_x\text{CoGe}$ alloys measured at room temperature, respectively. It can be seen that the crystal structure changes from the coexistence of TiNiSi-type and Ni₂In-type structures to the single Ni₂In-type structure with the substitution of Fe for Co or Mn atoms. This indicates the martensitic transformation temperatures of the two series of alloys decrease from higher temperature down to lower temperature. The substitution of Fe for Mn or Co can effectively change the phase stability of MnCoGe alloys.

Indexing the XRD pattern of the $\text{Mn}_{0.97}\text{Fe}_{0.03}\text{CoGe}$ alloy (not shown in Fig.1(b)), the lattice parameters of Ni₂In-type hexagonal austenitic and TiNiSi-type orthorhombic martensitic phase were obtained. For austenitic structure, the lattice parameters are $a = 4.0812 \text{ \AA}$, $c = 5.289 \text{ \AA}$, and those of martensitic structure are $a = 5.9074 \text{ \AA}$, $b = 3.8178 \text{ \AA}$, $c = 7.0445 \text{ \AA}$, respectively. The unit-cell volume increases by 4.2% during the martensitic transformation, indicating a large lattice

distortion. This large and positive volume expansion can result in significant difference of atomic surrounding and crystal structure between Ni₂In-type and TiNiSi-type structures.

It is known that the radius of Fe (0.172 nm) is larger than that of Co atom (0.167 nm) while smaller than that of Mn atom (0.179 nm)^[35]. In Ni₂In-type structure, however, the main peaks of two series of alloys both shift to the large-angle direction with the substitution of Fe for Mn or Co atoms, which means the unit-cell sizes of the two series of alloys all decrease with the increasing of Fe content. In MnCo_{1-x}Fe_xGe alloys, the newly introduced Fe atoms will occupy Co sites since both MnCoGe and MnFeGe are isostructural^[36]. Thus the strong covalent effect between Fe and Ge atoms formed. The reduction of lattice parameter can be ascribed to this enhanced covalent effect, which just like the case in Fe-doped MnNiGe alloys^[18].

The temperature dependence of magnetization for MnCo_{1-x}Fe_xGe and Mn_{1-x}Fe_xCoGe alloys measured under a magnetic field of 100 Oe were shown in Fig.2 (a) and (b), respectively. It can be seen that the martensitic transformation temperature decreases with the substitution of Fe for Co or Mn atoms, which means the doping of Fe atoms can realize the desired coupling of martensitic structural transition and magnetic transition. This effect is very similar to the case in isostructural Fe-doped MnNiGe alloys^[18], in which the doping of Fe for transition-metal atoms can also effectively decrease the martensitic transition temperature to magnetic ordering temperature. In Mn_{1-x}V_xCoGe^[21] and MnNi_{1-x}Co_xGe_{1.05}^[23] alloys, the researchers attributed this effect to the so-called “chemical pressure”, originating from the different atom radii during substitution. The “chemical pressure” works like the applied external hydrostatic pressure to tune the phase stability^[26]. In this work, the substitution of Fe (0.172 nm) for Co (0.167 nm) or Mn (0.179 nm) atoms can give rise to the local lattice distortion in MnCo_{1-x}Fe_xGe and Mn_{1-x}Fe_xCoGe alloys, consequently imposing a similar “chemical pressure” effect and modifying the relative stability between the austenitic and martensitic phases. In nature, the “chemical pressure” corresponds to the local chemical bonding in these alloys. In Fe-doped MnCoGe alloys, as demonstrated in Fe-doped MnNiGe alloys^[18], the strengthened covalent bonding between the nearest-neighbor Fe and Ge atoms with respect to the nearest-neighbor Mn/Co and Ge atoms increases the stability of Ni₂In-type austenite structure and consequently decreases the martensitic transformation temperature.

The thermomagnetization curves of the MnCo_{0.94}Fe_{0.06}Ge and Mn_{0.97}Fe_{0.03}CoGe alloys in a

magnetic field up to 50 KOe are shown in the insets of Fig.2 (a) and (b), respectively. Due to the PM/FM-type martensitic transformation, the magnetization difference values for the two alloys are about 51 and 58 emu/g, respectively, which is closed to that of $\text{Mn}_{1-x}\text{CoGe}$ ^[17]. This magnetization difference may give rise to the magnetic-field-induced martensitic transformation and the large magnetic-entropy changes in the two series of alloys around room temperature.

Meanwhile, comparing the thermomagnetization curves of $\text{MnCo}_{0.94}\text{Fe}_{0.06}\text{Ge}$ with $\text{Mn}_{0.97}\text{Fe}_{0.03}\text{CoGe}$ alloys under 100 Oe and 50 KOe, we can find that their martensitic starting transition temperatures were pushed upward about 10 K by a magnetic field of 50 kOe, which implies a magnetic-field-induced martensitic transformation occurs. This also suggests that the stability of martensitic phase can be enhanced with the aid of applied external magnetic field.

Collecting the magnetic measurement data, the structural and magnetic phase diagrams for $\text{MnCo}_{1-x}\text{Fe}_x\text{Ge}$ and $\text{Mn}_{1-x}\text{Fe}_x\text{CoGe}$ alloys are both shown in Fig. 3. By alloying isostructural MnFeGe or FeCoGe compounds into MnCoGe, two interesting results can be observed as follows:

(i) In the present change range of composition, the Curie temperatures of austenite phase (T_C^A) and martensite phase (T_C^M) remain almost constant and they are basically at 276 K and 355 K, respectively, which are consistent with those of MnCoGe alloy^[9, 11, 17]. (ii) The martensitic transformation temperature is lowered, spanning over T_C^A and T_C^M . These two achievements subsequently result in a temperature window with an interval width of about 80 K between T_C^A and T_C^M . In this temperature window, the martensitic transformations with large magnetization difference can occur in $\text{Mn}_{1-x}\text{Fe}_x\text{CoGe}$ ($x \leq 0.05$) and $\text{MnCo}_{1-x}\text{Fe}_x\text{Ge}$ ($x \leq 0.06$) alloys.

In what follows, the magnetoresponse properties of $\text{MnCo}_{1-x}\text{Fe}_x\text{Ge}$ and $\text{Mn}_{1-x}\text{Fe}_x\text{CoGe}$ alloys are presented. The isothermal magnetization ($M-H$) curves of $\text{MnCo}_{0.94}\text{Fe}_{0.06}\text{Ge}$ and $\text{Mn}_{0.97}\text{Fe}_{0.03}\text{CoGe}$ alloys were measured in the process of increasing and decreasing magnetic field up to 50 KOe across the temperature windows. These results are shown in Fig.4 (a) and (b), respectively. For both alloys, their magnetizations show similar changes under the applied magnetic field in the temperature windows. Above the T_m , the magnetization linearly increases with the increase of magnetic field, which indicates the PM ground state of Ni_2In -type structure. While below the T_m , the two alloys with TiNiSi -type structure show typical FM behavior. Around

the T_m , an S-shaped metamagnetic transition with a hysteresis indicates the occurrence of the remarkable magnetic-field-induced martensitic transformation from PM austenite to FM martensite. This is due to the larger Zeeman energy in the FM martensite introduced by the applied external magnetic field^[3, 4, 17].

Based on the isothermal magnetization curves, the magnetic-entropy changes for $\text{MnCo}_{0.94}\text{Fe}_{0.06}\text{Ge}$ and $\text{Mn}_{0.97}\text{Fe}_{0.03}\text{CoGe}$ alloys were estimated by Maxwell relation^[37], as shown below, and shown in Fig.5 (a) and (b), respectively.

$$\Delta S_m(T, H) = \int_0^H \left(\frac{\partial M(T, H)}{\partial T} \right)_H dH \quad (1)$$

For $\text{MnCo}_{0.94}\text{Fe}_{0.06}\text{Ge}$ and $\text{Mn}_{0.97}\text{Fe}_{0.03}\text{CoGe}$ alloys, the largest magnetic-entropy changes (ΔS_m) are about -27.5 and -10.6 J/Kg·K under the applied magnetic field of 50 KOe around the martensitic transformation temperature, respectively. Apparently, compared with $\text{MnCo}_{0.94}\text{Fe}_{0.06}\text{Ge}$ alloy, the $\text{Mn}_{0.97}\text{Fe}_{0.03}\text{CoGe}$ alloy shows a relatively smaller magnetic-entropy change in a wide temperature range. And the value of magnetic-entropy change of $\text{MnCo}_{0.94}\text{Fe}_{0.06}\text{Ge}$ alloy can be comparable with the those of $\text{Mn}_{1-x}\text{CoGe}$ (-26 J/Kg·K for $\Delta H=50$ kOe)^[17], $\text{Ni}_{52.6}\text{Mn}_{23.1}\text{Ga}_{24.3}$ (-18.0 J/Kg·K for $\Delta H=50$ kOe)^[38] and $\text{Ni}_{50}\text{Mn}_{33.13}\text{In}_{13.90}$ (28.6 J/Kg·K for $\Delta H=50$ kOe)^[39]. These negative ΔS_m values in this work can be ascribe to the first-order ferromagnetic martensitic transformation from high-temperature PM austenite to the low-temperature FM martensite. Importantly, just like the case in Fe-doped MnNiGe alloys, these martensites are in a more ferromagnetic ordered state after the phase transition, which results in a large ΔS_m value in Fe-doped MnCoGe alloys. Thus, for $\text{MnCo}_{0.94}\text{Fe}_{0.06}\text{Ge}$ and $\text{Mn}_{0.97}\text{Fe}_{0.03}\text{CoGe}$ alloys, the large and negative ΔS_m values around room temperature enables them to be potential magnetoresponse materials. For the difference of magnetic-entropy changes between $\text{MnCo}_{0.94}\text{Fe}_{0.06}\text{Ge}$ and $\text{Mn}_{0.97}\text{Fe}_{0.03}\text{CoGe}$, it can be ascribed to their different magnetization behavior under the same magnetic field. As shown in Fig.2(a) and (b), the martensitic transformation of $\text{MnCo}_{1-x}\text{Fe}_x\text{Ge}$ in a narrower temperature range is sharper than that of $\text{Mn}_{1-x}\text{Fe}_x\text{CoGe}$ alloys, which corresponds to higher value of $\left(\frac{\partial M(T, H)}{\partial T} \right)_H$. Thus, based on Maxwell relation, the ΔS_m of $\text{MnCo}_{1-x}\text{Fe}_x\text{Ge}$ alloys is higher than those of $\text{Mn}_{1-x}\text{Fe}_x\text{CoGe}$ alloys.

4. Conclusion

The crystal structure, ferromagnetic martensitic transformation and magnetoresponse properties of $\text{MnCo}_{1-x}\text{Fe}_x\text{Ge}$ and $\text{Mn}_{1-x}\text{Fe}_x\text{CoGe}$ alloys have been investigated in this work. Using isostructural alloying method, the martensitic transformation from Ni_2In -type structure to TiNiSi -type structure can be lowered down to the magnetic ordering temperatures of the two series of alloys. A Curie-temperature window can be uncovered by substituting of Fe for Co or Mn.

The desired PM/FM-type magnetostructural transition, accompanied with a large magnetization difference, can be thus realized in this temperature window between T_C^M and T_C^A . The remarkable magnetic-field-induced martensitic transformation and the large and negative magnetic-entropy changes around room temperature were observed in $\text{MnCo}_{0.94}\text{Fe}_{0.06}\text{Ge}$ and $\text{Mn}_{0.97}\text{Fe}_{0.03}\text{CoGe}$ alloys.

ACKNOWLEDGMENT

This work is supported by the National Natural Science Foundation of China (Grant Nos. 11174352 and 50901043) and National Basic Research Program of China (973 Program: 2012CB619405).

References

- ¹ K. Ullakko, J. K. Huang, C. Kantner, R. C. O'Handley, V. V. Kokorin, *Appl. Phys. Lett.* **69** (1996) 1966.
- ² G. H. Wu, C. H. Yu, L. Q. Meng, J. L. Chen, F. M. Yang, S. R. Qi, W. S. Zhan, Z. Wang, Y. F. Zheng, L. C. Zhao, *Appl. Phys. Lett.* **75** (1999) 2990.
- ³ R. Kainuma, Y. Imano, W. Ito, Y. Sutou, H. Morito, S. Okamoto, O. Kitakami, K. Oikawa, A. Fujita, T. Kanomata, K. Ishida, *Nature* **439** (2006) 957.
- ⁴ S. Y. Yu, Z. H. Liu, G. D. Liu, J. L. Chen, Z. X. Cao, G. H. Wu, B. Zhang, X. X. Zhang, *Appl. Phys. Lett.* **89** (2006) 162503.
- ⁵ J. M. Barandiarán, V. A. Chernenko, P. Lázpita, J. Gutiérrez, J. Feuchtwanger, *Phys. Rev. B* **80** (2009) 104404.
- ⁶ T. Krenke, E. Duman, M. Acet, E. F. Wassermann, X. Moya, L. Manosa, A. Planes, *Nat. Mater.* **4** (2005) 450.
- ⁷ O. Gutfleisch, M. A. Willard, E. Bruck, C. H. Chen, S. G. Sankar, J. P. Liu, *Adv. Mater.* **23** (2011) 821.
- ⁸ L. Castelliz, *Monatsh. Chem.* **84** (1953) 765.
- ⁹ V. Johnson, *Inorg. Chem.* **14** (1975) 1117
- ¹⁰ A. Szytuła, A. T. Pedziwiatr, Z. Tomkowicz, W. Bażela, J. Magn. Mater. **25** (1981) 176.
- ¹¹ W. Jeitschko, *Acta Crystallogr. B* **31** (1975) 1187.
- ¹² K. Koyama, M. Sakai, T. Kanomata, K. Watanabe, *Jpn J. Appl. Phys.* **1** **43** (2004) 8036.
- ¹³ J. T. Wang, D. S. Wang, C. F. Chen, O. Nashima, T. Kanomata, H. Mizuseki, Y. Kawazoe, *Appl. Phys. Lett.* **89** (2006) 262504.
- ¹⁴ C. L. Zhang, D. H. Wang, Q. Q. Cao, Z. D. Han, H. C. Xuan, Y. W. Du, *Appl. Phys. Lett.* **93** (2008) 122505.
- ¹⁵ K. Morrison, J. D. Moore, K. G. Sandeman, A. D. Caplin, L. F. Cohen, *Phys. Rev. B* **79** (2009) 5.
- ¹⁶ C. L. Zhang, D. H. Wang, Q. Q. Cao, Z. D. Han, H. C. Xuan, Y. W. Du, *J. Phys. D-Appl. Phys.* **42** (2009) 4.

- 17 E. K. Liu, W. Zhu, L. Feng, J. L. Chen, W. H. Wang, G. H. Wu, H. Y. Liu, F. B. Meng, H. Z.
Luo, Y. X. Li, *EPL* **91** (2010) 17003.
- 18 E.K. Liu, W.H. Wang, L. Feng, W. Zhu, G.J. Li, J.L. Chen, H.W. Zhang, G.H. Wu, Ch.B. Jiang,
H.B. Xu, F. R. d. Boer, *Nat. Commun.* **3** (2012) 873.
- 19 E.K. Liu, Y. Du, J.L. Chen, W.H. Wang, H.W. Zhang, G. H. Wu., *IEEE Trans. Magn.* **47** (2011)
4041.
- 20 T. Samanta, I. Dubenko, A. Quetz, S. Temple, S. Stadler, N. Ali, *Appl. Phys. Lett.* **100** (2012)
052404.
- 21 S. C. Ma, Y. X. Zheng, H. C. Xuan, L. J. Shen, Q. Q. Cao, D. H. Wang, Z. C. Zhong, Y. W. Du,
J. Magn. Magn. Mater. **324** (2012) 135.
- 22 N. T. Trung, V. Biharie, L. Zhang, L. Caron, K. H. J. Buschow, E. Brück, *Appl. Phys. Lett.* **96**
(2010) 162507.
- 23 C.L. Zhang, D.H. Wang, Q.Q. Cao, S.C. Ma, H.C. Xuan, Y. W. Du, *J. Phys. D-Appl. Phys.* **43**
(2010) 205003.
- 24 J. B. A. Hamer, R. Daou, S. Özcan, N. D. Mathur, D. J. Fray, K. G. Sandeman, *J. Magn. Magn.
Mater.* **321** (2009) 3535.
- 25 N. T. Trung, L. Zhang, L. Caron, K. H. J. Buschow, E. Brück, *Appl. Phys. Lett.* **96** (2010)
172504.
- 26 L. Caron, N. T. Trung, E. Brück, *Phys. Rev. B* **84** (2011) 020414.
- 27 S. Nizioł, A. Zięba, R. Zach, M. Baj, L. Dmowski, *J. Magn. Magn. Mater.* **38** (1983) 205.
- 28 S. Anzai, K. Ozawa, *Phys. Rev. B* **18** (1978) 2173.
- 29 H. Luo, F. Meng, Z. Feng, Y. Li, W. Zhu, G. Wu, X. Zhu, C. Jiang, H. Xu, *J. Appl. Phys.* **107**
(2010) 013905.
- 30 Z. H. Liu, M. Zhang, W. Q. Wang, W. H. Wang, J. L. Chen, G. H. Wu, F. B. Meng, H. Y. Liu,
B. D. Liu, J. P. Qu, Y. X. Li, *J. Appl. Phys.* **92** (2002) 5006.
- 31 K. Fukushima, K. Sano, T. Kanomata, H. Nishihara, Y. Furutani, T. Shishido, W. Ito, R. Y.
Umetsu, R. Kainuma, K. Oikawa, K. Ishida, *Scripta Mater.* **61** (2009) 813.
- 32 A. Manzoni, K. Chastaing, A. Denquin, P. Vermaut, J. van Humbeeck, R. Portier, *Scripta
Mater.* **64** (2011) 1071.
- 33 V. Provenzano, A. J. Shapiro, R. D. Shull, *Nature* **429** (2004) 853.
- 34 S. Lin, O. Tegus, E. Bruck, W. Dagula, T. J. Gortenmulder, K. H. J. Buschow, *IEEE Trans.
Magn.* **42** (2006) 3776.
- 35 <http://www.zdic.net/appendix/f7.htm>.
- 36 A. Szytula, A. T. Pedziwiatr, Z. Tomkowicz, & W. Bażęła, *J. Magn. Magn. Mater.* **25**
(1981) 176.
- 37 L. Caron, Z. Q. Ou, T. T. Nguyen, D. T. Cam Thanh, O. Tegus, E. Brück, *J. Magn. Magn.
Mater.* **321** (2009) 3559.
- 38 F. X. Hu, B. G. Shen, J. R. Sun, G. H. Wu, *Phys. Rev. B* **64** (2001) 132412.
- 39 X. X. Zhang, B. Zhang, S. Y. Yu, Z. H. Liu, W. J. Xu, G. D. Liu, J. L. Chen, Z. X. Cao, G. H.
Wu, *Phys. Rev. B* **76** (2007) 132403.

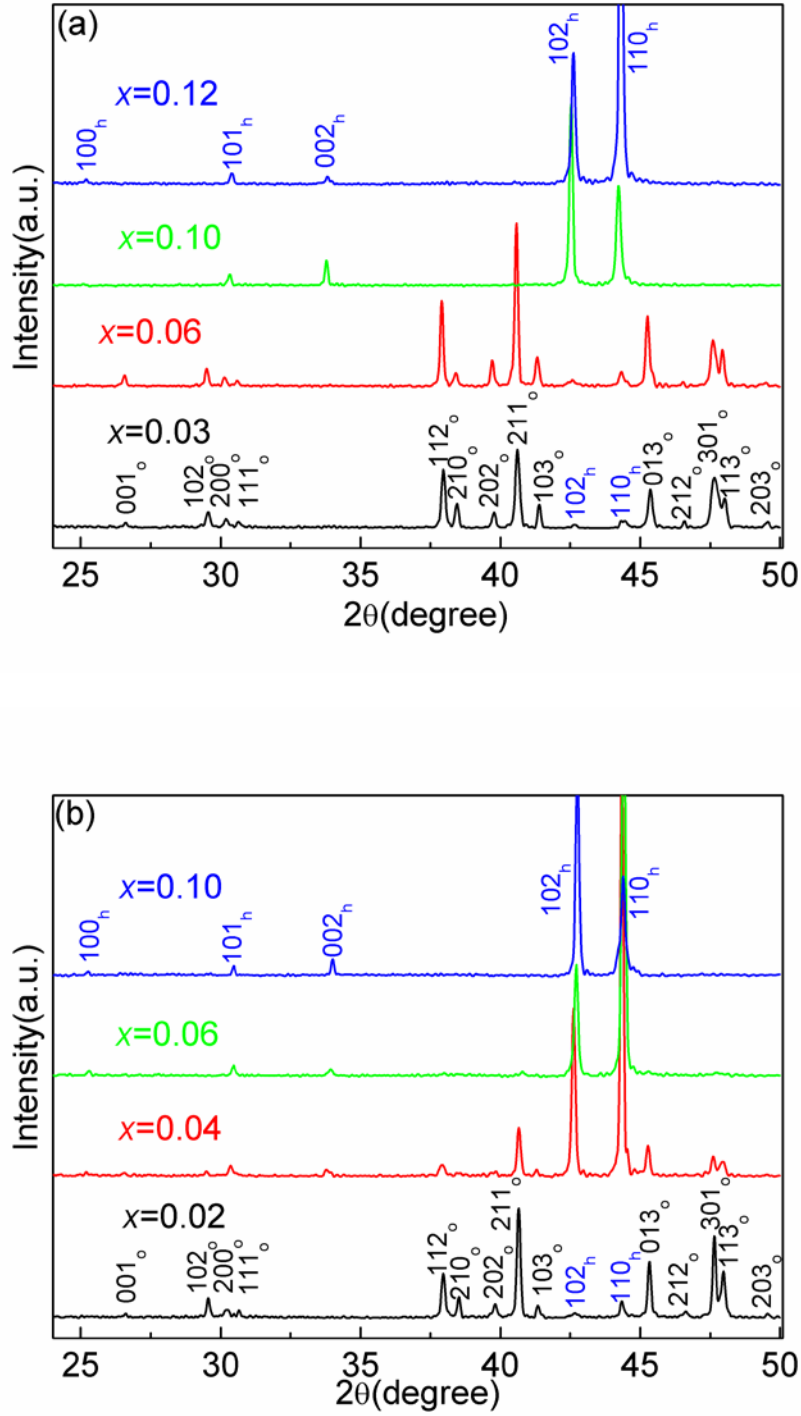


Fig.1. (Color online) XRD patterns of MnCo_{1-x}Fe_xGe alloys ($x = 0.03, 0.06, 0.10, 0.12$) (a) and Mn_{1-x}Fe_xCoGe alloys ($x = 0.02, 0.04, 0.06, 0.10$) (b). Here h and o denote the Ni₂In-type hexagonal and TiNiSi-type orthorhombic structures, respectively.

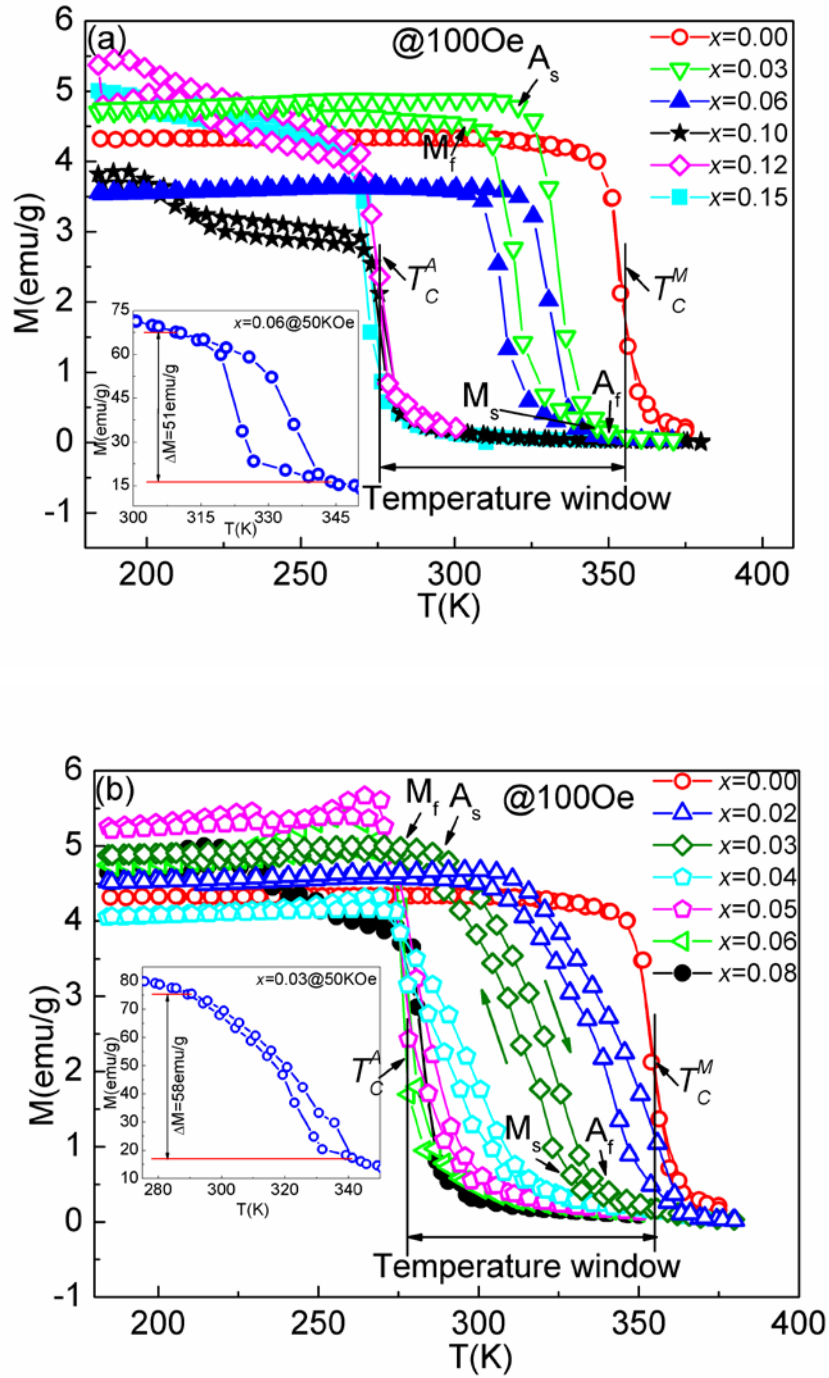


Fig.2. (Color online) Temperature dependence of magnetization of MnCo_{1-x}Fe_xGe alloys (a) and Mn_{1-x}Fe_xCoGe alloys (b) measured under a magnetic field of 100 Oe. Insets of (a) and (b) show the temperature dependence of magnetization of MnCo_{0.94}Fe_{0.06}Ge and Mn_{0.97}Fe_{0.03}CoGe alloys under a magnetic field of 50 kOe, respectively. M_s and M_f denote the starting and finishing temperatures of the martensitic transformation; A_s and A_f are the starting and finishing temperatures of the reverse transformation.

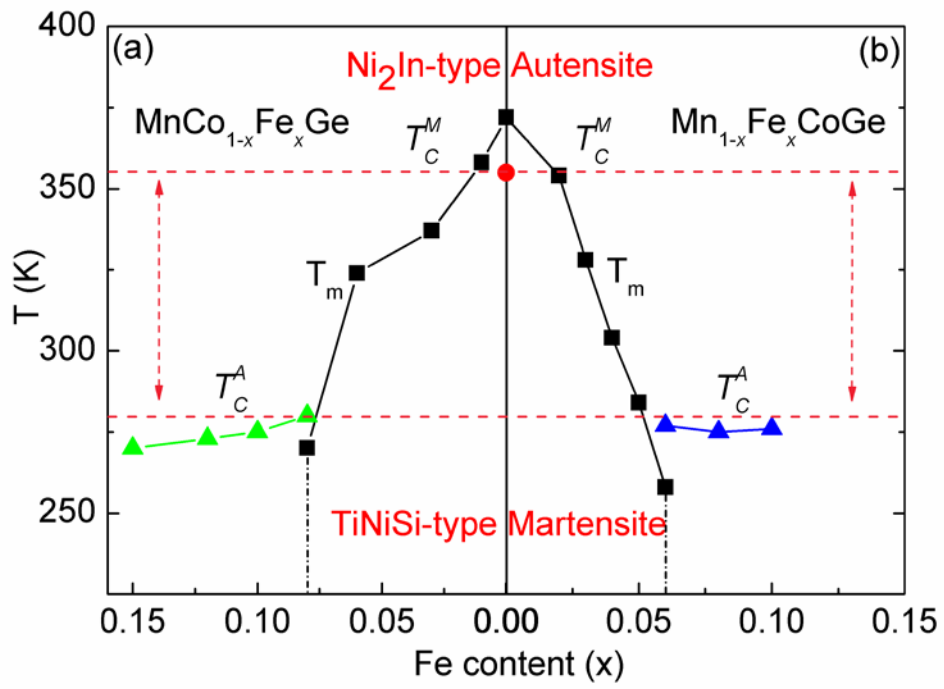


Fig.3. (Color online) Structural and magnetic phase diagram of $\text{MnCo}_{1-x}\text{Fe}_x\text{Ge}$ (a) and $\text{Mn}_{1-x}\text{Fe}_x\text{CoGe}$ alloys (b).

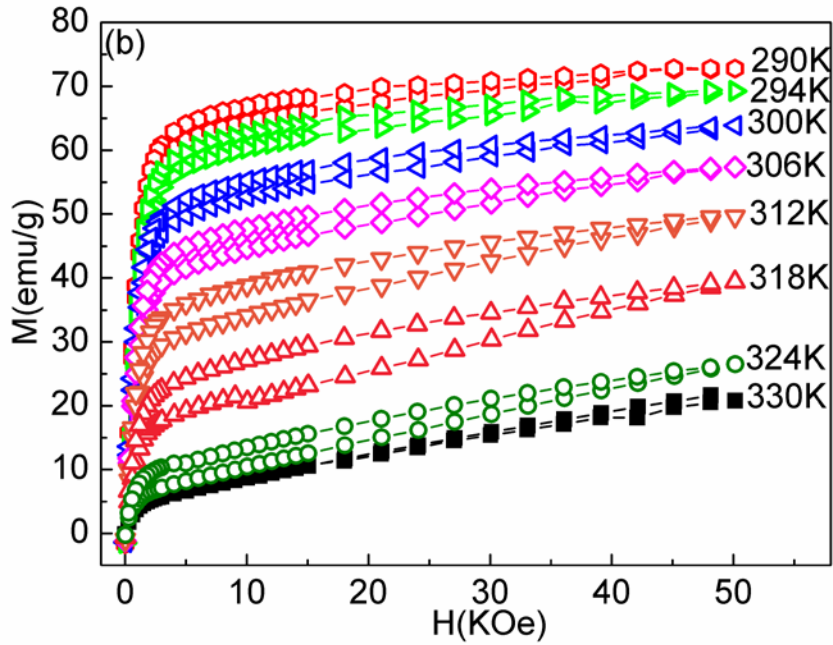
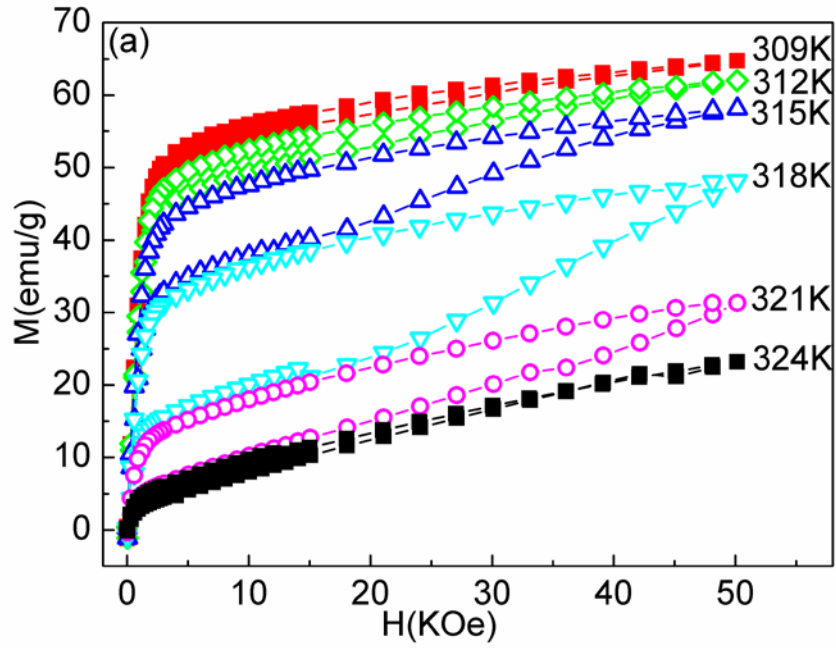


Fig.4. (Color online) Isothermal magnetization curves of the $\text{MnCo}_{0.94}\text{Fe}_{0.06}\text{Ge}$ (a) and $\text{Mn}_{0.97}\text{Fe}_{0.03}\text{CoGe}$ (b) alloys at various temperatures across the martensitic transformation in a magnetic field up to 50 kOe.

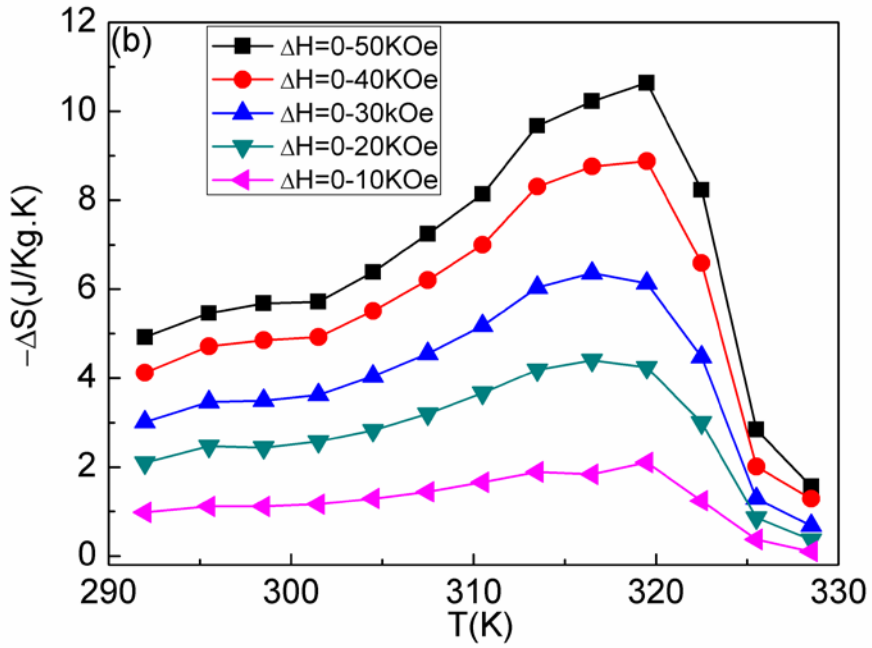
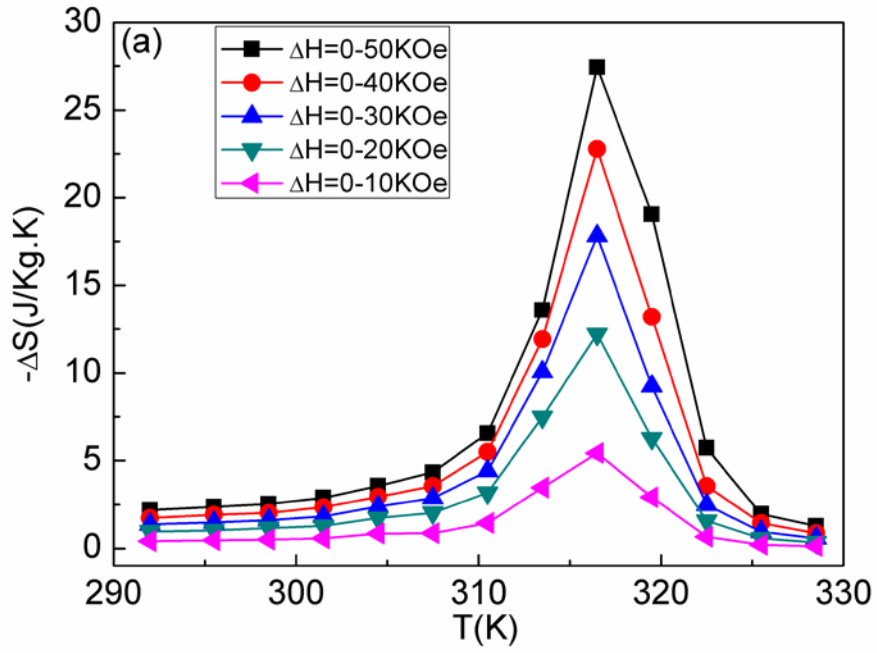


Fig.5. (Color online) Isothermal magnetic-entropy changes derived from isothermal magnetization curves of $\text{MnCo}_{0.94}\text{Fe}_{0.06}\text{Ge}$ (a) and $\text{Mn}_{0.97}\text{Fe}_{0.03}\text{CoGe}$ alloys (b).